

Vibration-Synchronized Magnetic Resonance Imaging for the Detection of Myocardial Elasticity Changes

Thomas Elgeti,¹ Heiko Tzschätzsch,¹ Sebastian Hirsch,¹ Dagmar Krefting,² Dieter Klatt,¹ Thoralf Niendorf,^{3,4} Jürgen Braun,² and Ingolf Sack^{1*}

Vibration synchronized magnetic resonance imaging of harmonically oscillating tissue interfaces is proposed for cardiac magnetic resonance elastography. The new approach exploits cardiac triggered cine imaging synchronized with extrinsic harmonic stimulation ($f = 22.83$ Hz) to display oscillatory tissue deformations in magnitude images. Oscillations are analyzed by intensity threshold-based image processing to track wave amplitude variations over the cardiac cycle. In agreement to literature data, results in 10 volunteers showed that endocardial wave amplitudes during systole (0.13 ± 0.07 mm) were significantly lower than during diastole (0.34 ± 0.14 mm, $P < 0.001$). Wave amplitudes were found to decrease 117 ± 40 ms before myocardial contraction and to increase 75 ± 31 ms before myocardial relaxation. Vibration synchronized magnetic resonance imaging improves the temporal resolution of magnetic resonance elastography as it overcomes the use of extra motion encoding gradients, is less sensitive to susceptibility artifacts, and does not suffer from dynamic range constraints frequently encountered in phase-based magnetic resonance elastography. Magn Reson Med 000:000–000, 2012. © 2012 Wiley Periodicals, Inc.

Key words: time harmonic vibrations; cardiac elastography; MRE; shear modulus; heart contraction; myocardial relaxation; shear waves

INTRODUCTION

Cardiac function is determined by the alteration of myocardial elasticity during the cardiac cycle. Therefore, measurement of myocardial elasticity may support the diagnosis and follow-up of cardiac contraction and relaxation abnormalities. Challenges for noninvasively mapping myocardial elasticity arise from the complex geometry of the heart, its periodic motion, structural anisotropy of the myocardium, and its pronounced viscoelastic and hyperelastic behavior (1). Various groups have tackled cardiac elasticity imaging by developing a variety of dedicated elastography methods (2–8). In gen-

eral, elastography requires mechanical stimulation of tissue, measurement of the induced tissue response, and extraction of diagnostic parameters from the acquired data. Cardiac magnetic resonance elastography (MRE) uses low-frequency mechanical oscillations for stimulating the heart through the anterior chest wall (6,8–10). The flux of elastic waves through the heart is captured by cardiac motion-synchronized phase-contrast magnetic resonance imaging (MRI) techniques (11,12). Phase-contrast-based MRE has recently been used for measuring cardiac volume–pressure cycles (13,14), isovolumetric tension-relaxation times of the heart (15), and symptomatically reduced diastolic relaxation (16).

In general, the MRI phase signal can encode coherent particle shifts on the order of microns (17,18). This inherent sensitivity to motion combined with the capability to encode motion in arbitrary directions renders MRI suitable for flow quantification and elastography. While in flow quantification particle velocity is measured, MRE is designed to capture deflection of the oscillating shear wave field assuming time-harmonic motions. Normally, the amplitudes of externally induced harmonic oscillations inside the body are low, i.e., on the order of tens of microns. Particularly at high shear wave frequencies larger than 80 Hz, viscose damping dominates in vivo vibration patterns. On the other hand, shear waves penetrate the body without any major attenuation at drive frequencies below 25 Hz. In this case, deflection amplitudes approach the order of millimeters throughout the body without the use of an excessive oscillation stimulus. With this low-frequency regime, the externally induced motion is in the order of the in-plane resolution commonly used in clinical MRI. Consequently, oscillations become directly visible in the morphological contrast of an MR image. The oscillatory response of tissue morphology to external stimuli measured by standard MRI may provide elastodynamic information without phase image processing and wave inversion. Unlike conventional MRE, the proposed method does not require specially tailored phase-contrast techniques for encoding oscillatory motion by extra motion-encoding gradients (MEG). Instead, any MRI sequence synchronized to externally induced tissue vibrations can be used motivating henceforth the term vibration-synchronized MRI (vsMRI). As no MEG is required in vsMRI, echo time and repetition time (TR) can be shortened reducing signal relaxation, susceptibility artifacts and improving temporal resolution in cine steady-state MRE. This study demonstrates the feasibility of vsMRI and examines its applicability for cardiac MRE. For this purpose, a

¹Department of Radiology, Charité—Universitätsmedizin Berlin, Campus Mitte, 10117 Berlin, Germany.

²Institute of Medical Informatics, Charité—Universitätsmedizin Berlin, Campus Benjamin Franklin, 12200 Berlin, Germany.

³Berlin Ultrahigh Field Facility (B.U.F.F.), Max-Delbrück Center for Molecular Medicine, 13125 Berlin, Germany.

⁴Experimental and Clinical Research Center, a joint cooperation between The Charité Medical Faculty and The Max-Delbrück Center for Molecular Medicine, Berlin, Germany.

*Correspondence to: Ingolf Sack, M.D., Department of Radiology, Charité—Universitätsmedizin Berlin, Campus Mitte, Charitéplatz 1, 10117 Berlin, Germany. E-mail: ingolf.sack@charite.de

Received 7 July 2011; revised 18 November 2011; accepted 5 January 2012.

DOI 10.1002/mrm.24185

Published online in Wiley Online Library (wileyonlinelibrary.com).

© 2012 Wiley Periodicals, Inc.

standard balanced steady-state imaging technique was synchronized with external, low-frequency stimulation to display endocardial oscillatory motion superimposed to intrinsic cardiac activity. The timing and the degree of wave amplitude alterations over the cardiac cycle is analyzed, and the results derived from vsMRI are compared with those previously reported by echocardiography and phase-based cardiac MRE.

Myocardial Mechanics Measured by Vibration Amplitudes

The basic idea of amplitude-sensitive cardiac elastography is the conservation of oscillatory strain energy in the heart wall during continuous time-harmonic excitation of shear waves. This concept, initially introduced in (8) implies a constant flux of elastic wave energy through the heart, i.e.,

$$\langle F \rangle = \langle E \rangle c = \text{const.} \quad [1]$$

$\langle F \rangle$ and $\langle E \rangle$ denote the time average of the flux of energy and energy density, while c represents the velocity of the “flow” of energy per unit area per unit time that is transported by the elastic waves. Assuming time-harmonic plane waves of amplitude U and angular driving frequency ω , the following relation can be obtained for the average of F over a wave oscillation period (19):

$$\langle F \rangle = \frac{1}{2} \rho c U^2 \omega^2 \quad [2]$$

where ρ is the material’s density. A more general field representation of the elastic wave intensity that allows for compression and transverse wave modes is given in the appendix of (8). Equation 2 shows that the time average of the intensity of the waves depends on both the wave velocity and the square of wave amplitude U . Thus, the ratio of U at two different time points, t_1 and t_2 , during the cardiac cycle is related to the inverse wave speed ratio and thus to the inverse ratio of the myocardial shear moduli μ :

$$\frac{U(t_2)}{U(t_1)} = \left(\frac{c(t_1)}{c(t_2)} \right)^{\frac{1}{2}} = \left(\frac{\mu(t_1)}{\mu(t_2)} \right)^{\frac{1}{4}}. \quad [3]$$

This equation provides the key relationship between vibration amplitudes and myocardial elasticity and has been applied in multiple studies of time-harmonic cardiac elastography using MRI (8,13–16) or ultrasound (20). Although the model seems simplistic considering the complexity of the beating heart, the myocardial mechanical parameters probed by shear wave amplitudes U have been proven physiologically consistent (13,14). In vsMRI, Eq. 3 provides the metric for deducing elasticity ratios from a single point in space (e.g., at the endocardial tissue interface), where vibration amplitudes are delineable in the magnitude image. It is notable that the spatial extension of the propagating wave is not measured, i.e., no quantitative elastic modulus is measured. Instead, we focus on the time function of relative modulus changes giving rise to relative changes in $U(t)$ according to Eq. 3. This article is about the exploitation of an

improved temporal resolution of $U(t)$ measured by vsMRI. The underlying key assumptions are:

- alteration of the myocardial shear modulus during the cardiac cycle
- no alteration of the myocardial compression modulus
- continuous flux of wave energy through the heart and applicability of Eq. 3
- the vibration component measured in a short axis view by vsMRI reveals similar information as previously gained by cardiac MRE accounting for the full vector field of motion.

The last point specifically applies to vsMRI. The rationale behind is the observation that the desired effect is seen in the anterior–posterior vibration component, which is in the direction of phase encoding (8).

MATERIALS AND METHODS

Subjects

The study was approved by the local institutional review board. Written informed consent was obtained from each volunteer. Ten healthy male volunteers were included in this study (mean age 34 ± 8.4 years, ranging from 23 to 46 years). None of the subjects had any history of cardiac events.

vsMRI

Experiments were performed on a clinical 1.5 T scanner (Siemens Magnetom Sonata, Erlangen, Germany). An extended piston driver was placed on the anterior chest wall to stimulate the heart with 22.83 Hz acoustic oscillations using a remote loudspeaker (13). The oscillations were synchronized with a balanced steady-state imaging sequence (bSSFP). Finger pulse oximetry was used for synchronization. Double oblique short axis views of the heart were acquired. As vsMRI does not require MEG short echo times are supported. This helps to reduce signal losses due to relaxation and improves temporal resolution in steady-state MRE. An echo time of 1.51 ms and a TR of 3.65 ms were achieved, so that one vibration period matched 12 TR. A total of 480 images were acquired. For each phase-encoding step, data acquisition was spread over 1.752 s (= 480 TR) to accomplish full R-R interval coverage. During this interval, a single phase-encoding step was performed for each image while continuously vibrating the chest by 40 cycles (= 480/12) of 22.83 Hz sinusoidal actuator motion. Matrix size was 256×192 with 400×300 mm² field of view, i.e., 1.56 mm in-plane resolution and 5 mm slice thickness. 2-fold acceleration using parallel imaging (GRAPPA reconstruction, 12 reference lines) lead to 108 phase-encoding steps. During each interval of data acquisition, the volunteers held their breath in expiration. This was followed by a short pause of 2.5 s used for one inspiration and expiration before the next k -line acquisition started (Fig. 1). Total imaging time was ~ 7.5 min, resulting from the 108 phase-encoding steps, each 4.25 s in duration (3.65 ms TR \times 480 images + 2.5 s delay for breathing). A flip angle of 65° was chosen to increase contrast

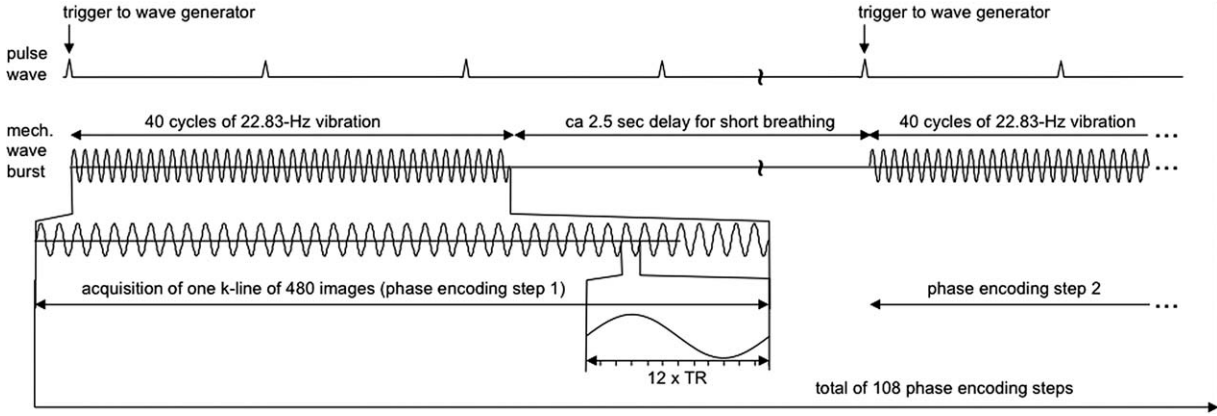


FIG. 1. Basic scheme of the vsMRI imaging technique. In this implementation, a pulse-wave-triggered and k -space-segmented bSSFP imaging sequence is synchronized with the external vibration. Twelve TR match one vibration period. Alternatively, bSSFP can be replaced by any imaging technique which provides appropriate blood/myocardium contrast and which supports a temporal resolution in the range of 3–4 ms.

between blood and myocardium (21). The contrast-to-noise ratio between blood and myocardium was calculated as the signal difference between both structures divided by standard deviation of noise (22).

Data Analysis

A vector \mathbf{r} of ~ 7 – 8 cm length running from the anterior chest wall through the short axis of the left ventricle was manually selected for each data set as illustrated in Fig. 2a. The intensity profiles $I(\mathbf{r})$ in all 480 bSSFP images were combined in a space-time matrix $I(\mathbf{r}, t)$ as demonstrated in Fig. 2b. Vibrations in the direction of \mathbf{x} (Fig. 3) were delineated by a processing routine applied to the space-time matrix $I(\mathbf{r}, t)$. Processing included (i) manual raw selection of the tissue interface of interest and (ii) automatic tracing of isolines of equal intensity I . As a result, a one-dimensional vibration function $u(t)$ was

obtained, which was analyzed in two ways. First, to determine the vibration amplitude, a Hilbert transform using a 5 Hz bandpass filter centered at the vibration frequency was applied and the vibration magnitude $U(t)$ was displayed. Second, to determine cardiac motion $u_0(t)$, the vibration was eliminated from $u(t)$ using a low-pass filter with 10 Hz cutoff frequency. $U(t)$ was corrected for possible projection biases of wave vector \mathbf{k} in the oblique view (Fig. 3). This amplitude correction is based on planar waves propagating from the actuator plate toward the heart with wave vector \mathbf{k} collinear to the anterior–posterior axis (the y -axis) in our coordinate system. The effective angle φ as shown in Fig. 3 depends on the angulation of the image slice and the position of profile \mathbf{r} relative to the position of the transducer. $U'(t)$ denotes the corrected wave magnitude with $U'(t) = \cos\varphi \cdot U(t)$. $U'(t)$ was measured in two anatomic regions: (i) at the body surface (U'_{surf}) encompassing a region

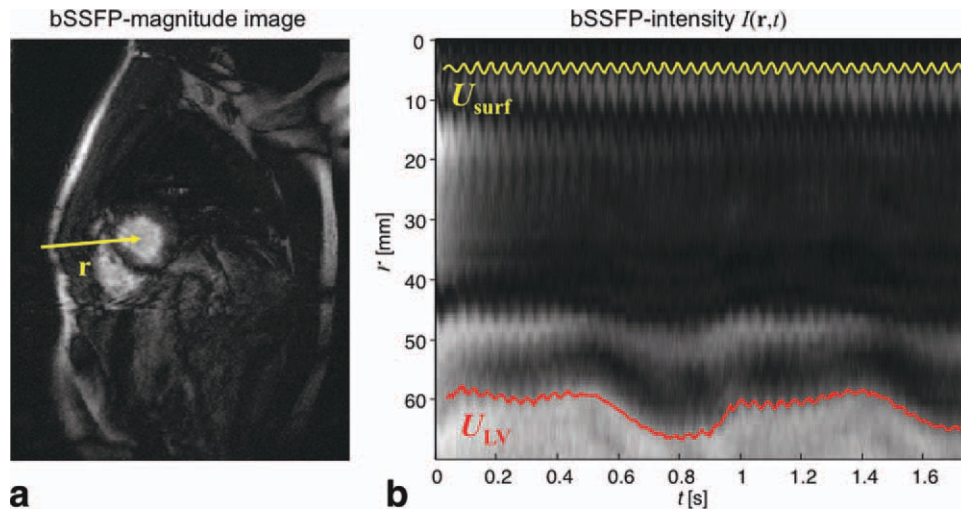


FIG. 2. a: Systolic short axis view of the heart using a magnitude image derived from a bSSFP acquisition to display cardiac anatomy and the position of profile \mathbf{r} . b: Profile \mathbf{r} shown in (a) plotted over time using a M-mode like view. Vibrations due to the externally induced 22.83 Hz motion are very well visible in the chest wall, the anterior heart boundary of the right ventricle, and the septum. In this study, we focused on vibrations of the endocardium (U_{LV}) in relation to systolic heart motion as well as vibrations delineated at the thorax surface (U_{surf}).

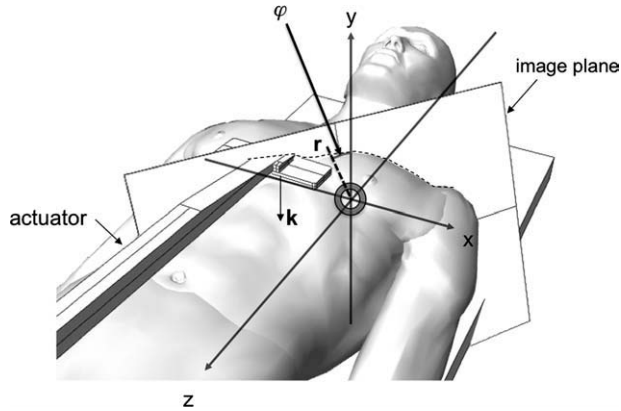


FIG. 3. For the estimation of the relative angle φ between profile \mathbf{r} and wave vector \mathbf{k} , a wave propagation direction along y (the anterior–posterior axis) was assumed. \mathbf{r} is within the image plane which intersects the heart in the short anatomical axis.

close to the position of the piston driver and (ii) at the anteriorseptal endocardium of the left ventricle (U'_{LV}). Systolic phases of the cardiac cycle were defined as inward movement of the left ventricular wall, whereas an outward movement of the myocardial wall characterized diastolic phases.

To estimate the temporal relationship between wave amplitude variation and motion of the myocardial wall, isovolumetric cardiac times were assessed using graphs of $u_0(t)$ superimposed to $U_{LV}(t)$. Isovolumetric contraction (IVC) was estimated by measuring the delay between descending slopes of $u_0(t)$ and $U_{LV}(t)$. Correspondingly, isovolumetric relaxation (IVR) was determined from the delay between the ascending branches of both functions. More specifically, the time instants t_1 and t_2 were selected from $U_{LV}(t_1) = U_{LV}(\text{systole}) + (U_{LV}[\text{diastole}] - U_{LV}[\text{systole}])/2$ and $u_0(t_2) = u_0(\text{systole}) + (u_0[\text{diastole}] - u_0[\text{systole}])/2$, which directly yield $\text{IVC} = t_2 - t_1$ at the descending branch of both graphs (in early systole) and $\text{IVR} = t_2 - t_1$ at the ascending branch (in early diastole). An illustration of t_1 and t_2 is given in (15). The isovolumetric cardiac times are compared with an age-matched

group of healthy volunteers investigated by phase-based cardiac MRE as reported in (15).

All data are given as mean \pm standard deviation. Student's t -test for paired samples was used to test systolic and diastolic wave amplitudes for statistical significance. The isovolumetric times derived from vsMRI and spin-phase-based MRE were compared by a two-sample Kolmogorov–Smirnov test. A P -value of < 0.05 was considered statistically significant.

RESULTS

Repetitive mechanical excitation during image acquisition followed by a short gate for shallow respiration was well tolerated by all volunteers without any adverse effects. Vibrations induced by the external actuator were visible in the thoracic wall, subcutaneous fat, and left ventricular myocardium as demonstrated in Fig. 3b.

The resolution of vsMRI to tissue deflection is determined by the contrast-to-noise ratio. The contrast-to-noise ratio of the myocardium–blood interface averaged over all images was on the order of 127. A change in the signal intensity of a pixel right at the myocardium–blood interface of larger than 127 would indicate a deflection of 1.56 mm. Therefore, $1.56 \text{ mm}/127 = 0.012 \text{ mm}$ can be considered as a theoretical spatial resolution limit for the experimental vsMRI setup described here.

Wave Amplitude of the Thoracic Wall

At the surface of the thoracic wall, the corrected vibration amplitude was $0.68 \pm 0.39 \text{ mm}$ (see Table 1), ranging between 0.25 and 1.45 mm. No change in amplitude related to the periodicity of the cardiac cycle was observed.

Wave Amplitude in the Left Ventricular Myocardium

The wave amplitude in the left ventricular myocardium showed a time varying difference between systolic and diastolic phase of the cardiac cycle as highlighted in Fig. 4. The mean corrected wave amplitude was $0.13 \pm 0.07 \text{ mm}$ during systole and $0.34 \pm 0.14 \text{ mm}$ during diastole

Table 1
Synopsis of results derived from vsMRI in 10 volunteers

Vol.#	φ ($^\circ$)	U'_{surf} (mm)	$U'_{LV(\text{sys})}$ (mm)	$U'_{LV(\text{dia})}$ (mm)	IVC (ms)	IVR (ms)	u_0 (mm)
1	51.7	0.25	0.06	0.22	86	54	5.7
2	49.0	0.28	0.13	0.37	120	35	5.0
3	48.9	0.40	0.09	0.20	93	75	4.0
4	50.7	0.50	0.04	0.19	177	108	4.0
5	46.7	0.48	0.17	0.52	177	32	6.5
6	45.7	0.70	0.18	0.43	98	95	7.0
7	49.9	1.45	0.26	0.61	110	110	8.0
8	47.8	0.94	0.15	0.31	93	73	7.0
9	49.7	1.11	0.10	0.23	178	162	4.0
10	34.4	0.66	0.08	0.33	175	113	6.0
Mean	47.4	0.68	0.13	0.34	131	86	5.7
SD	4.9	0.39	0.07	0.14	41	40	1.4

The effective angle φ is between the profiles \mathbf{r} and the AP-axis in the scanner system, which is assumed to be collinear with the wave normals. Wave amplitudes U'_{surf} , $U'_{LV(\text{sys})}$, and $U'_{LV(\text{dia})}$ correspond to amplitude values corrected for geometrical overestimation by multiplying measured wave magnitude $U(t)$ with $\cos\varphi$. The subscripts identify the location of measurement (surf = thoracic surface, LV = left ventricle) and time of measurement (sys = systolic phase, dia = diastolic phase). IVC and IVR denote the delay between change in wave amplitude U_{LV} and heart motion u_0 at the myocardial wall.

($P < 0.001$, Table 1). The mean ratio between diastolic and systolic wave amplitudes averaged over all volunteers in vsMRI was 2.9 ± 0.9 (range 1.7–4.3). The inward movement of the left ventricle during systole was 5.7 ± 1.4 mm.

Cardiac Time Intervals

Alteration in myocardial wave amplitude started 117 ± 40 ms before myocardial contraction, which defines our IVC-time, and 75 ± 31 ms before diastolic dilatation, which corresponds to our IVR-time. Data of phase-based cardiac MRE from an age-matched subgroup published previously (15) shows a mean IVC-times of 130 ± 19 ms (range 101–161 ms) and a mean IVR-time of 83 ± 22 ms (range 51–120 ms), respectively. IVC- and IVR-times derived showed no significant difference ($P = 0.68$ and 0.31, respectively).

DISCUSSION

Our results demonstrate the feasibility of vsMRI for cardiac elastography. In this study, vsMRI replaces the MEG in phase-based methods with a faster morphological-based scanning method. A 12.5-min scan in (8) is replaced with a 7.5-min scan with improved temporal (factor of 1.6) and spatial resolution (factor of 1.6 without interpolation in the phase-encode direction). The induced vibration clearly appears as oscillation of tissue boundaries in the magnitude image. The induced vibration can be analyzed with image processing methods tailored for motion tracking. Our main finding is that a periodic change in wave amplitude $U_{LV}(t)$ can be observed ahead of the periodic cardiac motion $u_0(t)$. The minimum detectable vibration amplitudes were below the spatial resolution in the MR image. Minor oscillatory deflections below voxel size can cause changes in partial volumes, resulting in changes in the magnitude signal analyzed by vsMRI. In our experience, vsMRI requires steady wave amplitudes at least in the order of one-tenth of the in-plane image resolution. This amplitude is approximately an order of magnitude larger than what is needed in conventional phase-based MRE.

The signal shift produced in vsMRE is related to the physical tissue displacement and not to intravoxel phase dispersion, which occurs in the case of a high displacement gradient throughout the voxel (23,24). As a consequence, vsMRE depends on the amplitude and not on the wave number of the induced tissue vibration. In contrast to intravoxel phase dispersion-based techniques, which rely on encoding phase incoherencies that deteriorate the magnitude signal, vsMRI displays coherent oscillatory shifts whose frequency can be arbitrarily low. Also, low vibration frequencies are beneficial as high wave amplitudes are achievable without exceeding the vibration safety limits (25). Admittedly, low vibration frequencies result in low wave numbers and hence require an alternative image analysis versus inversion-based reconstruction of classical MRE (26,27).

To our knowledge, there are three major concepts in MRE that use low-frequency deformations: (i) static or quasi-static MRE (11,28), (ii) scatter-based MRE (29), and (iii) steady-state MRE for cardiac applications (8,13).

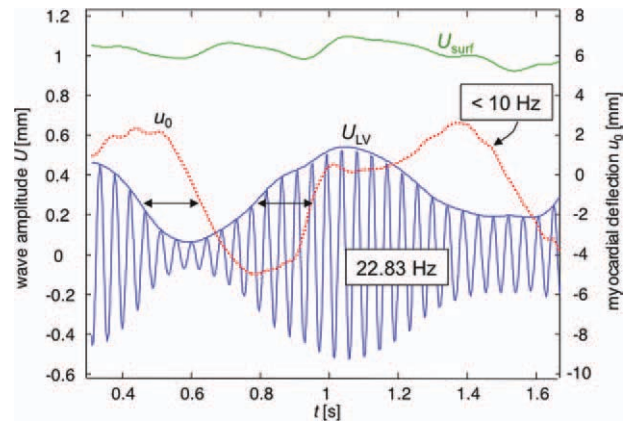


FIG. 4. Time course of wave amplitudes detected at the surface (green) and in the left ventricular myocardium (blue). The movement of the left ventricular wall is displayed in red. No wave amplitude alterations periodic to the cardiac cycle are observed for the thoracic wall surface. The wave amplitude in the left ventricle changes with respect to the cardiac phase. The change in wave amplitude is ahead of heart motion, giving rise to IVC and IVR times (indicated by arrows). [Color figure can be viewed in the online issue, which is available at wileyonlinelibrary.com.]

In this study, only the latter was exploited with the focus on the principal relationship of coherent tissue oscillations $U(t)$ observed at the interfaces: The wave amplitude measured on the thoracic surface showed no variation with respect to the cardiac cycle. At the endocardial border, however, the wave amplitudes varied in synchrony with the cardiac phases. The observed delay between alteration of wave amplitudes and myocardial motion (117 ± 40 ms in early systole and 75 ± 31 ms in early diastole) strongly indicates that vsMRI can separate myocardial elastodynamics from heart morphology. The isovolumetric times measured by vsMRI are not significantly different from phase-contrast-based steady-state cardiac MRE (15) while differences exist to (8), which are due to different methods of determining IVC and IVR from the superposition of $u_0(t)$ and $U_{LV}(t)$. Compared with echocardiography, elasticity-based IVC-times as measured by MRE seem to be considerably longer (63 ± 14 ms vs. 131 ± 41 ms) (30). As discussed in (15), this effect might be attributed to the elastic properties of muscle tissue being nonlinear under large deformation, rendering the measured MRE wave response stretch-dependent. Such nonlinear behavior would predominantly occur during ventricular dilatation, i.e., during early systole when myocardial tissue is at its maximum prestretch.

It is an intriguing result of this study that vsMRI was able to reproduce the time intervals without consideration of the vector nature of the displacement field. In phase-based cardiac MRE, the direction of motion sensitization is varied in consecutive runs, as the resulting displacement amplitude is calculated from three Cartesian displacement components. In vsMRI, the variation of systolic and diastolic wave amplitude was 2.9 ± 0.9 . Equation 3 allows one to calculate a relative change of the shear modulus by $\sim (2.9)^4 = 70.7$. This value is in good agreement with the ratio derived from phase-based

MRE. It is notable that in phase-based MRE, the largest effect of wave amplitude modulation is observed along the in-plane vibration direction that virtually points from the actuator toward the heart (see Fig. 4 in (8)). The profiles chosen in vsMRI can be considered to resemble the deflection component along the in-plane vibration direction of phase-based MRE.

Future studies including a broad range of cardiac pathologies have to be conducted to determine which diagnostic parameters can be derived by vsMRI. Admittedly, vsMRI is limited by the requirement of image contrast between tissue components, blood/myocardium contrast in our case, which is used for delineating motion patterns. The use of balanced SSFP provides blood and myocardium contrast, which is superior to that of gradient echo techniques (21). The endocardial region examined here seems to be particularly suited for cardiac vsMRI. It can be well delineated due to the high myocardium/blood contrast. Also, pathophysiological reasons support the use of the endocardial regions because disturbances of myocardial metabolism first affect endocardial perfusion, which in turn impacts the relaxation and contraction of the heart in that region (31).

For future developments, a two-dimensional cross-correlation method capable of tracking the in-plane vector components of left ventricular deformation could facilitate data analysis. Vibration synchronized MRI may also be tested as a method for quasi-static MRE using rapid imaging techniques—for instance single-shot echo planar imaging—in at least two different vibration phases combined with subsequent nonaffine image registration for the assessment of tissue strain.

In conclusion, vsMRI combines high-amplitude coherent tissue oscillations with synchronized MR imaging for monitoring the oscillation of tissue interfaces. The method proposed in this feasibility study provides the same high spatial and temporal resolution achieved with state-of-the-art MRI techniques. vsMRI does not require extra MEG. With vsMRI, elasticity-based differences in wave amplitude between cardiac systole and diastole can be measured in healthy volunteers.

REFERENCES

- Fung Y-C. Biomechanics. New York: Springer; 1993.
- Konofagou EE, D'hooge J, Ophir J. Myocardial elastography—a feasibility study in vivo. *Ultrasound Med Biol* 2002;28:475–482.
- Bouchard RR, Hsu SJ, Wolf PD, Trahey GE. In vivo cardiac, acoustic-radiation-force-driven, shear wave velocimetry. *Ultrasound Imaging* 2009;31:201–213.
- Kanai H. Propagation of spontaneously actuated pulsive vibration in human heart wall and in vivo viscoelasticity estimation. *IEEE Trans Ultrason Ferroelectr Freq Control* 2005;52:1931–1942.
- Nenadic IZ, Urban MW, Mitchell SA, Greenleaf JF. Lamb wave dispersion ultrasound vibrometry (LDUV) method for quantifying mechanical properties of viscoelastic solids. *Phys Med Biol* 2011;56:2245–2264.
- Robert B, Sinkus R, Gennisson J-L, Fink M. Application of DENSE-MR-elastography to the human heart. *Magn Reson Med* 2009;62:1155–1163.
- Kolipaka A, Mcgee KP, Araoz PA, Glaser KJ, Manduca A, Romano AJ, Ehman RL. MR elastography as a method for the assessment of myocardial stiffness: comparison with an established pressure-volume model in a left ventricular model of the heart. *Magn Reson Med* 2009;62:135–140.
- Sack I, Rump J, Elgeti T, Samani A, Braun J. MR elastography of the human heart: noninvasive assessment of myocardial elasticity changes by shear wave amplitude variations. *Magn Reson Med* 2009;61:668–677.
- Rump J, Klatt D, Braun J, Warmuth C, Sack I. Fractional encoding of harmonic motions in MR elastography. *Magn Reson Med* 2007;57:388–395.
- Kolipaka A, Araoz PA, Mcgee KP, Manduca A, Ehman RL. Magnetic resonance elastography as a method for the assessment of effective myocardial stiffness throughout the cardiac cycle. *Magn Reson Med* 2010;64:862–870.
- Plewes DB, Betty I, Urchuk SN, Soutar I. Visualizing tissue compliance with MR imaging. *J Magn Reson Imaging: JMRI* 1995;5:733–738.
- Muthupillai R, Lomas DJ, Rossman PJ, Greenleaf JF, Manduca A, Ehman RL. Magnetic resonance elastography by direct visualization of propagating acoustic strain waves. *Science* 1995;269:1854–1857.
- Elgeti T, Rump J, Hamhaber U, Papazoglou S, Hamm B, Braun J, Sack I. Cardiac magnetic resonance elastography. Initial results. *Invest Radiol* 2008;43:762–772.
- Elgeti T, Laule M, Kaufels N, Schnorr J, Hamm B, Samani A, Braun J, Sack I. Cardiac MR elastography: comparison with left ventricular pressure measurement. *J Cardiovasc Magn Reson* 2009;11:44.
- Elgeti T, Beling M, Hamm B, Braun J, Sack I. Elasticity-based determination of isovolumetric phases in the human heart. *J Cardiovasc Magn Reson* 2010;12:60.
- Elgeti T, Beling M, Hamm B, Braun J, Sack I. Cardiac magnetic resonance elastography: toward the diagnosis of abnormal myocardial relaxation. *Invest Radiol* 2010;45:782–787.
- Moran PR. A flow velocity zeugmatographic interlace for NMR imaging in humans. *Magn Reson Imaging* 1982;1:197–203.
- Feinberg DA, Crooks L, Hoenninger J, Arakawa M, Watts J. Pulsatile blood velocity in human arteries displayed by magnetic resonance imaging. *Radiology* 1984;153:177–180.
- Achenbach JD. Wave propagation in elastic solids. Amsterdam: Elsevier; 1999.
- Tzschätzsch H, Elgeti T, Rettig K, Klaua R, Schultz M, Kargel C, Braun J, Sack I. In vivo time harmonic elastography of the human heart. *Ultrasound Med Biol* 2012;38:214–222.
- Scheffler K, Lehnhardt S. Principles and applications of balanced SSFP techniques. *Eur Radiol* 2003;13:2409–2418.
- Huber A, Bauner K, Wintersperger BJ, Reeder SB, Stadie F, Mueller E, Schmidt M, Winnik E, Reiser MF, Schoenberg SO. Phase-sensitive inversion recovery (PSIR) single-shot TrueFISP for assessment of myocardial infarction at 3 tesla. *Invest Radiol* 2006;41:148–153.
- Glaser KJ, Felmlee JP, Manduca A, Ehman RL. Shear stiffness estimation using intravoxel phase dispersion in magnetic resonance elastography. *Magn Reson Med* 2003;50:1256–1265.
- Glaser KJ, Felmlee JP, Manduca A, Kannan Mariappan Y, Ehman RL. Stiffness-weighted magnetic resonance imaging. *Magn Reson Med* 2006;55:59–67.
- Ehman EC, Rossman PJ, Kruse SA, Sahakian AV, Glaser KJ. Vibration safety limits for magnetic resonance elastography. *Phys Med Biol* 2008;53:925–935.
- Manduca A, Oliphant TE, Dresner MA, Mahowald JL, Kruse SA, Amromin E, Felmlee JP, Greenleaf JF, Ehman RL. Magnetic resonance elastography: non-invasive mapping of tissue elasticity. *Med Image Anal* 2001;5:237–254.
- Papazoglou S, Hamhaber U, Braun J, Sack I. Algebraic Helmholtz inversion in planar magnetic resonance elastography. *Phys Med Biol* 2008;53:3147–3158.
- Chenevert TL, Skovoroda AR, O'Donnell M, Emelianov SY. Elasticity reconstructive imaging by means of stimulated echo MRI. *Magn Reson Med* 1998;39:482–490.
- Papazoglou S, Xu C, Hamhaber U, Siebert E, Bohner G, Klingebiel R, Braun J, Sack I. Scatter-based magnetic resonance elastography. *Phys Med Biol* 2009;54:2229–2241.
- Spencer K. Age dependency of the Tei index of myocardial performance. *J Am Soc Echocardiogr* 2004;17:350–352.
- Vitanis V, Manka R, Giese D, Pedersen H, Plein S, Boesiger P, Kozerke S. High resolution three-dimensional cardiac perfusion imaging using compartment-based k - t principal component analysis. *Magn Reson Med* 2011;65:575–587.